Journal of Pharmaceutical and Biomedical Analysis 131 (2016) 464–472

Contents lists available at ScienceDirect

Journal of Pharmaceutical and Biomedical Analysis

journal homepage: www.elsevier.com/locate/jpba

Pharmacokinetic properties, *in vitro* metabolism and plasma protein binding of govaniadine an alkaloid isolated from *Corydalis govaniana* Wall

Lucas M.M. Marques[a], Daniel R. Callejon[a], Larissa G. Pinto[a,b], Michel L. de Campos[c], Anderson R.M. de Oliveira[d], Ricardo Vessecchi[d], Achyut Adhikari[e], Ram L.S. Shrestha[f], Rosangela G. Peccinini[c], Norberto P. Lopes[a,*]

[a] *Departamento de Físico-Química, Faculdade de Ciências Farmacêuticas de Ribeirão Preto, Universidade de São Paulo, 14040-903 Ribeirão Preto, São Paulo, Brazil*
[b] *Wolfson Centre for Age-Related Diseases, Kings College London, Guy's Campus, London Bridge, SE11UL—London, England*
[c] *Faculdade de Ciências Farmacêuticas de Araraquara, Departamento de Princípios Ativos Naturais e Toxicologia, Universidade Estadual Paulista Júlio de Mesquita Filho, 14801-902 Araraquara, São Paulo, Brazil*
[d] *Departamento de Química, Faculdade de Filosofia, Ciências e Letras de Ribeirão Preto, Universidade de São Paulo, 14040-901 Ribeirão Preto, São Paulo, Brazil*
[e] *HEJ Research Institute of Chemistry, International Center for Chemical and Biological Sciences, University of Karachi, Karachi 75270, Pakistan*
[f] *Amrit Science Campus, Tribhuvan University, Kathmandu, Nepal*

ARTICLE INFO

Article history:
Received 31 May 2016
Received in revised form 30 August 2016
Accepted 1 September 2016
Available online 3 September 2016

Keywords:
Govaniadine
in vitro metabolism
Pharmacokinetics
Two-compartment model

ABSTRACT

Govaniadine (GOV) is an alkaloid isolated from *Corydalis govaniana* Wall. It has been reported to show a different number of biological activities including anti-urease, leishmanicidal and antinociceptive. The present study aims to characterize the GOV *in vitro* metabolism after incubation with rat and human liver microsomes (RLM and HLM, respectively) and to evaluate its pharmacokinetic properties. The identification of GOV metabolites was conducted by different mass analyzers: a micrOTOF II—ESI-ToF Bruker Daltonics® and an amaZon-SL *ion trap* (IT) Bruker Daltonics®. For the pharmacokinetic study of GOV in rats after intravenous administration, a LC–MS/MS method was developed and applied to. The analyses were performed using an Acquity UPLC® coupled to an Acquity TQD detector equipped with an ESI interface. The liver microsomal incubation resulted in new O-demethylated, di-hydroxylated and mono-hydroxylated compounds. Regarding the method validation, the calibration curve was linear over the concentration range of 2.5–3150.0 ng mL^{-1}, with a lower limit of quantitation (LLOQ) of 2.5 ng mL^{-1}. This method was successfully applied to a pharmacokinetic study. The profile was best fitted to a two-compartment model, the first phase with a high distribution rate constant (α) 0.139 ± 0.086 min^{-1}, reflected by the short distribution half-life ($t1/2\alpha$) 9.2 ± 8.9 min and the later one, with an elimination half-life ($t1/2\beta$) 55.1 ± 37.9 min. The main plasma protein binding was 96.1%. This is a first report in this field and it will be useful for further development of govaniadine as a drug candidate.

1. Introduction

Natural products (NPs) form a rather heterogeneous class of compounds differentiated by their biological role and source organisms: plants, bacteria, yeast, fungi and marine organisms to name a few. They have historically been a significant source for lead compounds or pharmacophores for medicinal chemistry and also play a key role in drug discovery due to their structural diversity, complexity and potential to show biological activities. Hence, they have been used as a bottom line in the development of clinical drugs [1–3].

The genus *Corydalis* (family Fumariaceae) is distributed mostly in Eurasia [4]. The plants from this genus have been used as analgesic and anticancer agents in east Asia [5] and alkaloids are considered the most important constituents responsible for biological activities [6]. Tetrahydroprotoberberine-type alkaloids are identified as a new category of dopamine receptor ligands and antimalarial agents [7].

* Corresponding author.
E-mail address: npelopes@gmail.com (N.P. Lopes).

http://dx.doi.org/10.1016/j.jpba.2016.09.003
0731-7085/

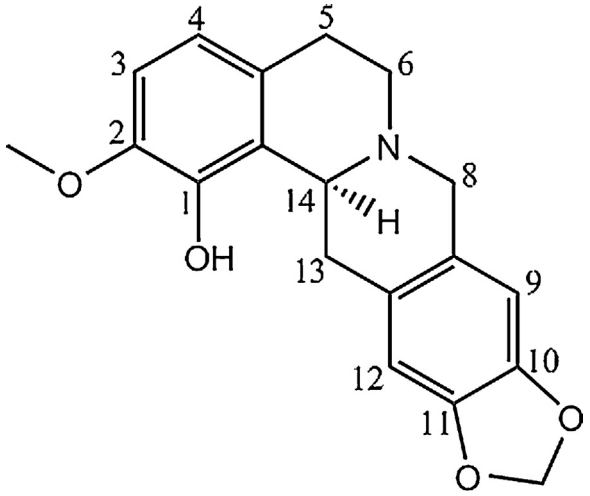

Fig. 1. Chemical structure of the govaniadine.

In this context, govaniadine (GOV, Fig. 1) is one of the main active constituent isolated from *Corydalis govaniana* Wall. [7], a glabrous herb distributed in the Himalayas of Nepal, Pakistan and India [4,7]. GOV has been reported to show a different number of biological activities including anti-urease [7], leishmanicidal [8] and antinociceptive [4]. These activities have inspired the conduction of a study regarding its pharmacokinetic profile and *in vitro* metabolism.

Pharmacokinetics and metabolism studies play a notable role in early drug discovery and development process [9]. Over the last decade, these studies have been responsible, for the decrease in the failure rate of drug development [10]. Obtaining the *in vivo* pharmacokinetic profile of a lead candidate in plasma over time enables a better correlation of its dosing regimen to its exposure and responses [11]. Furthermore, xenobiotic compounds are targets for metabolic biotransformation, mainly cytochrome P450 enzyme (CYP450s) mediated. Since such transformation may produce compounds with different pharmacological properties or reactive ones [12], GOV metabolism requires clarification, considering its previously mentioned activities.

Therefore, the purpose of the present study was to propose, to compare and to characterize the potential *in vitro* metabolites of govaniadine from incubation with pooled rat and human liver microsomes (RLM and HLM, respectively) and to evaluate its pharmacokinetic properties using high performance liquid chromatography coupled to mass spectrometer (LC–MS). Considering there have been no studies, in this field, for govaniadine, such work will be helpful to promote its further development as a drug.

2. Material and methods

2.1. Chemicals and reagents

The whole plant of *Corydalis govaniana* Wall. was collected from Langtang (Rashuwa, Nepal) and identified by Mr. Sanjiv Kumar Rai, Taxonomist, Department of Plant Resources, Thapathali (Kathmandu, Nepal). A voucher specimen, CG-207, has been deposited in Central Department of Botany, Tribhuvan University, Kirtipur (Kathmandu, Nepal). The extraction and isolation of Govaniadine ((14aS)-2-methoxy-5,8,14,14a-tetrahydro-6H-[1,3]dioxolo[4,5-g]isoquino[2,1-b]isoquinolin-1-ol) from *Corydalis govaniana* Wall. was previously published [7]. Mianserin (MIAN) was employed as internal standard (IS) (Sigma–Aldrich, Steinhein, Germany).

Acetonitrile (MeCN), chloroform ($CHCl_3$), ethyl acetate (EtOAc), methanol (MeOH), *n*-hexane (*n*-hex) and formic acid (CH_2O_2) were purchased from J.T. Baker (Phillipsburg, NY, USA). Water was purified using a Milli-Q system (Millipore, Bedford, USA). Sodium chloride and sodium dihydrogen phosphate were obtained from Merck (Darmstadt, Germany). Sodium hydroxide and potassium chloride were obtained from Nuclear (São Paulo, Brazil). Tris (hydroxymethyl) aminomethane was obtained from J.T. Baker. Nicotinamide adenine dinucleotide phosphate (NADPH), glucose-6-phosphate and glucose-6-phosphate dehydrogenase were obtained from Sigma–Aldrich (St. Louis, MO, USA). All other chemicals and reagents were of the highest analytical grade available.

Human liver microsomes (HLM, pooled mixed gender, fifty individual donors), NADPH regenerating system (NRS) Solution A (26.1 mM $NADP^+$, 66 mM glucose-6-phosphate, and 66 mM $MgCl_2$ in H_2O) and Solution B (40 U mL^{-1} glucose-6-phosphate dehydrogenase in 5 mM sodium citrate) were purchased from Corning Life Sciences (New York, NY, EUA). Rat liver microsomes (RLM, pooled from 6 animals) were obtained by differential high-speed centrifugation according to a previously published procedure [13]. All care and handling of the animals were performed with the approval of the Ethical Committee from the University of Sao Paulo (#14.1.721.53.6). The animal studies were performed in accordance with the Guiding Principles for Research Involving Animals and Human Beings from the American Physiological Society.

2.2. LC–MS/MS for metabolite identification

The identification of GOV metabolites was conducted using two Shimadzu (Kyoto, Japan) High Performance Liquid Chromatography (HPLC) each one coupled to different mass analyzers: a micrOTOF II—ESI-ToF Bruker Daltonics® (Billerica, MA, USA) and an amaZon-SL *ion trap* (IT) Bruker Daltonics®. The HPLC comprising a LC-20AD solvent pump unit, a CTO-20A column oven, a DGU-$20A_3$ online degasser, a CBM-20A system controller and a SPD-M20A (190 a 800 nm) diode array detector. Injections were performed automatically (5 μL) through a 100 μL loop SIL-20A HT. The separation of GOV and its metabolites was performed at 40 °C using a Kinetex™ XB-C18 Phenomenex column (100 mm × 2.1 mm d.i., 2.6 μm particle size) and a Phenomenex C18 column (2.0 mm × 2.1 mm d.i.) as guard column (Torrance, CA, USA.). The mobile phase was comprised of water (solvent A) and acetonitrile (solvent B) both with 0.1% formic acid, and it was pumped at a flow rate of 0.3 mL min^{-1}. The gradient elution program was performed as follows: 0–5 min 10% (B), 5–6 min 30% (B), 6–7 min 100% (B), 7–7.5 min 100% (B), 7.5–11 min 10% (B). For the high-resolution ToF (time-of-flight) analyzer, the mass spectrometer source parameters were set as follow: capillary voltage at 3.5 kV. Nitrogen (N_2) was used as nebulizing and drying gas (4 bar, 9 L min^{-1}, 200 °C). The electrospray ionization source (ESI) was operated in the positive ion mode. The detection was made considering a mass range of 100–500 *m/z*. The accurate masses were obtained by using sodiated trifluoroacetic acid (Na^+-TFA) as mass standard (10 mg mL^{-1}). The data were processed through Bruker Compass Data Analysis 4.1 software (Bremen, Germany). For the ion trap analyzer, the mass spectrometer source parameters were set as previously described and the data were processed on the same previous software.

2.3. In vitro metabolism

2.3.1. Rat liver microsome incubation

GOV (60 μmol L^{-1}) was added to sodium phosphate buffer (100 mmol L^{-1}; pH 7.4) containing rat liver microsomes (RLM, 1.0 mg microsomal protein mL^{-1} of incubation) and the mixture was pre-incubated using a shaking water bath at 37 °C for 5 min (model SL 157, Solab, Brazil). The reaction was initiated by adding

cofactor solution consisted of $NADP^+$ (0.25 mmol L^{-1}), glucose-6-phosphate (5 mmol L^{-1}) and glucose-6-phosphate dehydrogenase (0.5 units mL^{-1}) in Tris–HCl buffer (Tris–HCl 0.05 mol L^{-1}–KCl 0.15 mol L^{-1}, pH 7.4). The final incubation volume was set at 1000 μL. The composition of the sample control was identical except that no cofactor solution was added to the solution. The incubation was ended after 90 min by the addition of chloroform (4000 μL). After that, the sample preparation was carried out according to Section 2.3.3.

2.3.2. Human liver microsome incubation

GOV (30 μmol L^{-1}) was added to potassium phosphate buffer (100 mmol L^{-1}; pH 7.4) containing human liver microsomes (HLM, 1.0 mg microsomal protein mL^{-1} of incubation). Prior to the addition of NRS, the samples were incubated using a shaking water bath at 37 °C for 5 min. The reaction was initiated by the addition of a NRS (1.3 mmol L^{-1} $NADP^+$, 3.3 mmol L^{-1} glucose-6-phosphate, 0.4 units L^{-1} glucose-6-phosphate dehydrogenase, and 3.3 mmol L^{-1} $MgCl_2$ in 100 mmol L^{-1} potassium phosphate buffer, pH 7.4). The final incubation volume was set at 200 μL. The composition of the sample control was identical to the previous incubations except that no NRS was added. The incubation was ended after 90 min by the addition of chloroform (1000 μL). After that, the sample preparation was carried out according to Section 2.3.3.

2.3.3. Liver microsome sample preparation

A liquid–liquid extraction (LLE) procedure was employed to extract GOV from the liver microsomes (RLM and HLM). After 90 min of incubation, chloroform was added to the samples. Then, the samples were vortexed for 20 s (model AP56 Phoenix, Brazil), shaked for 15 min (Vibrax VXR agitator; IKA, Staufen, Germany) and centrifuged for 8 min at 3000 rpm (Hitachi CF16RXII, Himac, Tokyo, Japan). The organic layer from RLM and HLM incubation samples were collected (3000 and 750 μL, respectively) and allowed to evaporate to dryness under a rotation vaccum concentrator (30 min; 35 °C; Analitica, Christ RVC2-18, São Paulo). After that, the residue was reconstituted in 200 μL of the mobile phase MeCN:H_2O (10:90 v/v), filtered through a 0.22 μm polytetrafluorethylene membrane (Millex, Millipore) and 5 μL was injected into the chromatography system. All experiments were performed in triplicate (n = 3).

2.4. LC–MS/MS for validation procedure and the pharmacokinetic study

The UPLC®-MS/MS analyses were performed using an Acquity UPLC (Waters, Milford, MA, USA) coupled to an Acquity TQD detector equipped with an ESI interface and an Acquity UPLC BEH C18 (Bridged Ethylsiloxane Hybrid; 2.1 × 50 mm, 1.7 μM) column protected by an Acquity UPLC Vanguard column of the same material. The mobile phase composition, the gradient elution program, the flow rate and the column temperature were the same as described above (Section 2.2). The samples were conditioned at 10 °C in the auto-sampler. The injection mode applied was the partial loop with needle overfill, using 5 μL of injection volume. Data were acquired by MassLynx V4.1 software and processed for quantification by QuanLynx V4.1 (Waters). The MS tune parameters used were 0.16 L/h for the collision gas (argon) flow at a pressure of $\approx 3.02 \times 10^{-3}$ mBar in the collision cell, and the desolvation gas (N_2) flow was 650 L/h. The source and desolvation temperature were 150 °C and 350 °C, respectively. A multiple reaction monitoring mode (MRM) was used for the quantification of the analytes in the positive ionization mode, the optimized values are depicted on Table 1.

Table 1
Compound dependent parameters for GOV and MIAN in MRM mode for UPLC®-MS/MS analysis.

Analyte	Capillary (kV)	MRM (*m*/*z*)	Cone (V)	Collision energy (eV)
Govaniadine	2.5	326 > 178	20	15
Mianserin	2.5	265 > 208	25	20

2.4.1. Method validation

A bioanalytical validation method was performed according to the EMEA guideline [14]. The GOV stock solution was prepared in methanol at 1000 μg mL^{-1}. Working solutions were prepared at concentration levels of 0.025; 0.05; 0.1; 0.2; 0.4; 1.1; 10.5; 21.0; 26.3 e 31.5 μg mL^{-1} by serial dilution of the primary stock solution with methanol. The IS stock solution (1000 μg mL^{-1}) was prepared in methanol and was further diluted with methanol to 5.5 μg mL^{-1}. All solutions were kept at −20 °C and brought to room temperature (25 ± 2 °C) before use. The calibration standards were prepared by spiking 10 μL of the corresponding working solutions mentioned above into 100 μL blank plasma to yield the concentrations of 2.5, 5.0, 10.0, 20.0, 40.0, 110.0, 1050.0, 2100.0, 2630.0, 3150.0 ng mL^{-1} for GOV and 550 ng mL^{-1} for the MIAN.

Calibration curves (n = 5) were obtained by spiking aliquots of 100 μL drug-free plasma samples with GOV standard solutions, using separately prepared stock solutions. The linearity of the proposed method was checked over the concentration range of 2.50–3150.0 ng mL^{-1}. The calibration curve was constructed by plotting the GOV/IS peak area versus GOV concentrations. The correlation coefficient (r) and linear regression equation were calculated using the weighted least-squares linear regression method ($1/x^2$ weighting factor). In addition, the linearity was assessed using an ANOVA lack of fit test, setting the p value to ≥0.1 with MINITAB Release software, version 14.1 (State College, PA, USA).

The selectivity of the method was assured by analyzing six individual sources of plasma blank. The absence of interfering components was accepted when the response was less than 20% of the lower limit of quantitation (LLOQ = 2.5 ng mL^{-1}) for GOV and 5% for the IS. To assess carry-over effect, blank samples were injected immediately after the highest calibration standard (2630.0 ng mL^{-1}). Carry-over should not be greater than 20% of the lower limit of quantification and 5% for the IS. Matrix effects were investigated using normal (n = 6), haemolysed (n = 3) and hyperlipidaemic (n = 3) plasma from individual rats. For GOV and IS, the matrix factor (MF) was calculated by the ratio of the peak area in the presence of matrix to the peak area in absence of matrix. The IS-normalized MF was calculated by dividing the MF of the GOV by the MF of the IS. The coefficient of variation (CV, %) of the IS-normalized MF calculated from the six lots of plasma should not be greater than 15%. The determination was done at the concentrations levels of 5.0 and 2630.0 ng mL^{-1}.

The precision describes the closeness of repeated individual measures of analyte and it was expressed as coefficient of variation (CV, %). Accuracy describes the closeness of the determined value obtained by the method to the nominal concentration of the analyte and it was expressed as the percent of deviation between the true and the measured value, i.e., relative error (RER, %) [14]. To assess within-run precision and accuracy, the plasma samples were spiked to achieve the GOV concentrations: 2.5, 5.0, 40.0, 1050.0, 2630.0 and 3150.0 ng mL^{-1} (n = 5). For between-run assays, plasma samples at the same above described concentrations were determined during the routine operation of the system over a period of three working days. To quantity the samples from the precision and accuracy assays, an analytical curve was constructed on the same day and was used for the quantification of each sample. The limits for the accuracy and precision assays were set at 15% for the

RER% and for the CV%. The lower limit of quantitation (LLOQ) was performed at govaniadine concentration of 2.50 ng mL^{-1}. The limits for the accuracy and precision of the LLOQ were set at 20%. To determine the absolute recovery, 100 μL of plasma samples (n = 5 for each concentration) were spiked at GOV concentrations 2.50, 40.0, 2630.0 and 3150.0 ng mL^{-1} and submitted to the LLE procedure. The obtained peak areas for the analytes in these samples were compared with the peak areas obtained by the direct analysis of pure solutions containing identical amounts of each compound, which were dissolved in the mobile phase. Recovery was expressed as the percentage of the amount extracted, and the coefficient of variation was determined.

Stability tests were conducted to evaluate the short and long term, freeze–thaw and autosampler stability for samples spiked at low (5.0 ng mL^{-1}) and high (2630.0 ng mL^{-1}) GOV concentration levels (n = 5), the quality control samples (QC). For long term stability, the results obtained with freshly prepared stock solution were compared with those results obtained using the stock standard solutions stored in the freezer for 10 days (−60 °C). For the short term stability, GOV plasma samples were kept at room temperature (25 ± 2 °C) during 6 and 12 h. For freeze and thaw stability the QC samples were stored and frozen in the freezer (−60 °C) and thereafter thawed at room temperature (25 ± 2 °C). After complete thawing, samples were refrozen again applying the same conditions. At each cycle, samples were frozen for 12 h before they are thawed. It was employed three cycles. For the autosampler stability, after the LLE procedure, the samples were placed in the autosampler and then injected 24 h later. The samples were considered stable when the relative error (RER, %) from the nominal concentration was within ±15% and when the CV was below 15%.

2.4.2. Pharmacokinetic study

Wistar male rats (250 ± 10 g) were provided by the animal facility of the University of São Paulo, Ribeirão Preto Campus (#14.1.721.53.6). For the experiments, the animals were fasted for twelve hours before treatment.

The GOV dose (1 mg kg^{-1}) intravenously administered to the animals was solubilized with ethanol, 20% v/v [15] and with phosphate buffer (137 mM NaCl, 2.7 mM KCl, 4.3 mM Na_2HPO_4 and 1.4 mM KH_2PO_4, pH 7.4). Blood samples (≈200 uL) were collected at 5, 10, 20, 30, 40, 60, 90, 120 and 180 min in heparinized tubes. After collection, the tubes were centrifuged (20 min, 4° C, 2000 rpm; BOECO Germany M-240R, Germany) and the plasma was separated and stored in a freezer at −60 °C until the sample preparation procedure.

For the plasma samples [16] a 100 μL aliquot of plasma sample was transferred into a eppendorf tube (2 mL, Axigen®, Union City, NJ, USA). To this aliquot, 10 μL IS (5,5 μg mL^{-1}) and 750 μL of ethyl acetate were added. After vortex-mixing for 2 min (Gehaka AV-2, São Paulo, Brazil) and centrifuging (10 min, 4 °C, 10000 rpm; Boeco Germany M-240R, Germany), the organic layer was separated (600 μL) and evaporated to dryness under a rotation vaccum concentrator (30 min; 35 °C; Analitica, Christ RVC2-18, São Paulo). The residue was reconstituted in 200 μL of mobile phase MeCN:H_2O (10:90 v/v), filtered through a 0.22 μm polytetrafluorethylene membrane (Millex, Millipore) and 5 μL was injected into the UPLC®-MS/MS system.

Pharmacokinetic parameters were calculated using compartmental analysis tool of validated WinNonlin 6.4 software (USA, licence code: 0127ADEA801A4C40B9B46878AEA120 9AE3). The GOV plasma concentration–time curve was found to be best described by a two-compartment disposition model with the weighting factor of 1/(Yhat*Yhat). The area under the concentration time curve ($AUC_{0\text{-}180}$) was calculated by linear trapezoidal rule. $AUC_{0\text{-}\infty}$ was calculated using the equation $AUC_{0\text{-}180} + Cp_{last}/\beta$. The rate constants (α and β) were estimated in fitting the biexponential model to the concentration *versus* times curves. The half-life of distribution ($t_{1/2}\alpha$) was calculated using the equation 0.693/α and the half-life of elimination ($t_{1/2}\beta$) was calculated using the equation 0.693/β. The mean residence time (MRT) was calculated as $AUMC_{0\text{-}\infty}/AUC_{0\text{-}\infty}$, where $AUMC_{0\text{-}\infty}$ is the area under the first moment curve (the AUC of a plot of the product of concentration (C) × time (t) *versus t*). The systemic clearance (Cl) and the distribution volume (V_d) were determined by the equations Cl = Dose/$AUC_{0\text{-}\infty}$ and V_d = Cl/β [17]. All the parameters were described as arithmetic mean ± standard deviation (SD).

2.4.3. Plasma protein binding

In vitro plasma protein binding (PPB) was studied by an ultrafiltration (UF) method [18]. GOV solution was added to blank rat plasma (300 μL) to achieve the concentrations of 5.0 and 2630.0 ng mL^{-1}. Incubations took place in a shaking water bath (model SL 157, Solab, Brazil) at 37 °C for 2 h to allow equilibration, then the samples were transferred to Amicon Ultra-0.5 mL centrifugal filters (Millipore, Billerica, MA) with molecular weight of 30.000 Da cut off, sealed with the attached cap and centrifuged at 10,000 rpm, for 30 min at 37 °C (BOECO Germany M-240R, Germany) and 100 μL of the original volume of plasma was collected as an ultrafiltrate. The sample clean up was performed as previously described in Section 2.4.2. All experiments were performed in triplicate (n = 3). The GOV non-specific binding (NSB) to the filter membrane of the UF apparatus was assessed using spiked aqueous solution instead of using spiked plasma. The NSB was estimated according to Eq. (1) [19]:

$$NSB = C_{AB} - C_{AA}/C_{AB} \quad (1)$$

where C_{AB} is the total drug concentration in aqueous solution before centrifugation and C_{AA} is the drug concentration in the aqueous solution filtrate after centrifugation.

Thereby, the NSB correction to estimate the PPB was made using Eqs. (2) and (3) [19]:

$$Fu = C_{UF}/[(1\text{-}NSB)C_{NP}] \quad (2)$$

$$PPB = 100(1\text{-}F_u) \quad (3)$$

where F_u is the free fraction, C_{UF} is the GOV concentration in the plasma ultrafiltrate, and C_{NP} is the nominal plasma concentration.

2.5. Computational studies

In order to avoid speculative protonation site localization and fragmentation, the mechanisms were done on the basis of the computational chemistry calculations using B3LYP/6–311 + +G(d,p) model [20] by using of the Gaussian 03 software. With a view to clarify the fragmentation under mass spectrometry analysis, all the geometries, enthalpies and Gibbs energies of neutral and protonated forms were obtained by the vibrational frequency analysis computed. With regard to suggest the modification at structure from metabolism, the relative energies were computated in same model.

3. Results and discussion

3.1. Govaniadine identification

The unchanged GOV showed a LC profile (Fig. 2) with a retention time at 5.40 min and an HRESI-MS spectrum which gave a protonated molecule $[M+H]^+$ at *m/z* 326.1393 ($[C_{19}H_{20}NO_4]^+$, 1.9 ppm). Fragmentation of the $[M+H]^+$ in the MS ion trap yielded product ions with *m/z* values of 178 and 163 (Figs. 3 and 4 A). Theoretical calculations were performed and the protonation sites for govaniadine and its metabolites were indicated as being the N atom, the most

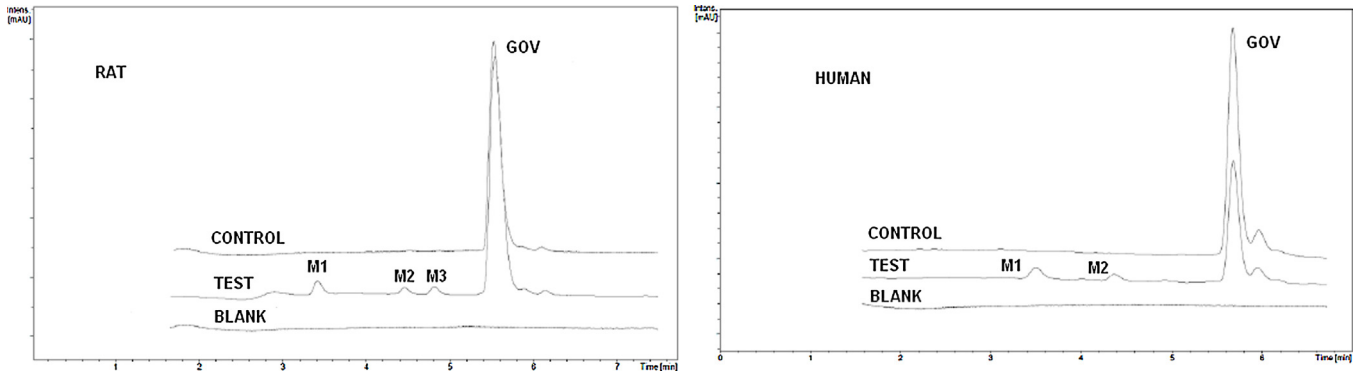

Fig. 2. HPLC chromatograms for GOV *in vitro* metabolism with rat and human liver microsomes. Legend: govaniadine (GOV), metabolite 1 (M1), metabolite 2 (M2) and metabolite 3 (M3).

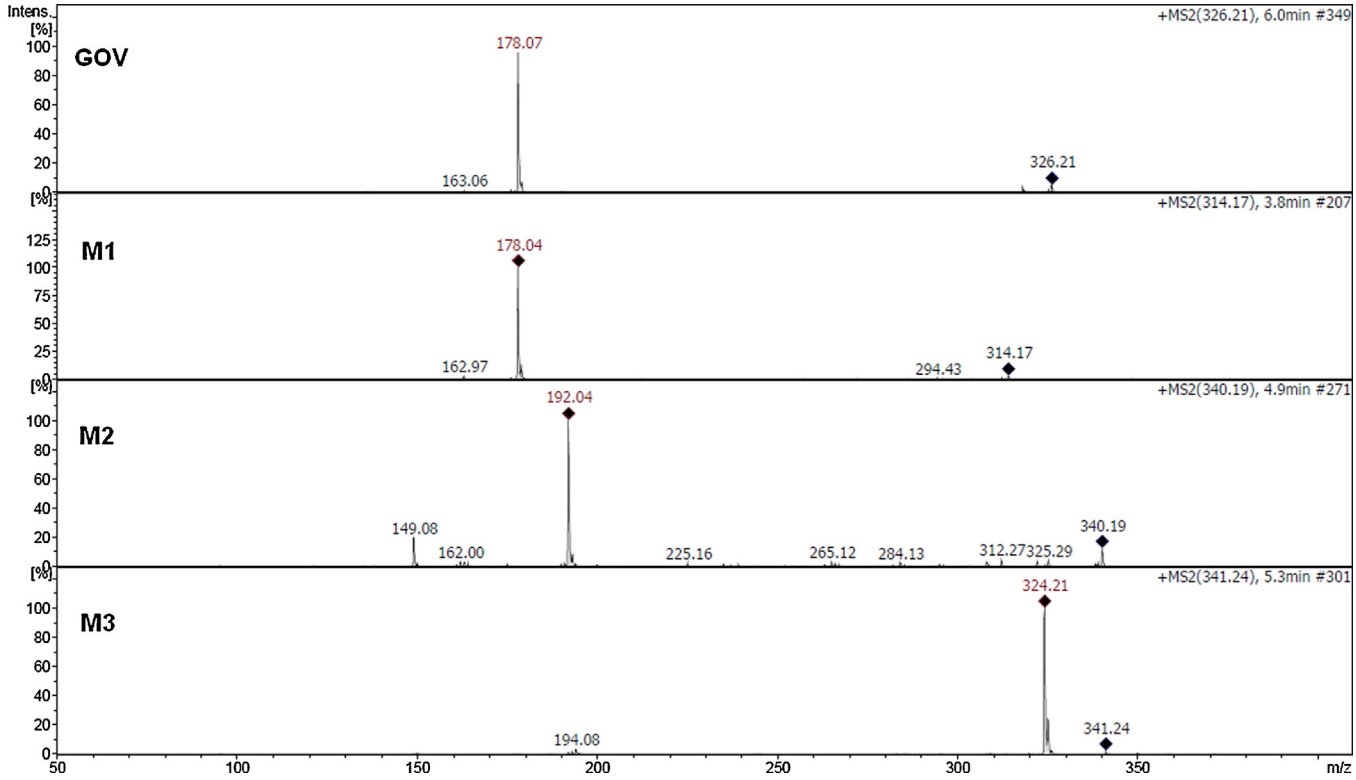

Fig. 3. Product mass spectra of $[M+H]^+$ ions of GOV, metabolite 1 (M1), metabolite 2 (M2) and metabolite 3 (M3).

basic site [Fig. S1 in the Supporting information (SI)]. Different protonation sites were tested, besides the values of proton affinity and basicities to be higher into N, for govaniadine, metabolite 1 (M1) and metabolite 2 (M2). Two pathways were observed regarding to the product ions (Fig. 4A). The one with *m*/*z* 178 is formed through Retro-Diels-Alder (RDA) fragmentation reaction. In addition, the fragment ion at *m*/*z* 163 was generated through the homolytic cleavage of the O—C bound resulting in a methyl radical loss from the methoxyl at C(2). This mechanism was very well described for mycosporins uplying theoretical and experimental analysis [21]. These fragmentation pathways are important to differentiate the possible modification into govaniadine after metabolism. Therefore, modifications on quinolin ring can influence the RDA reactions and, the *m*/*z* differences can indicate the occurred reaction.

3.2. Metabolite identification

Determination of *in vitro* metabolic profile of a compound plays a crucial role in understanding its metabolic pathway *in vivo* [22]. Liver microsomes are widely employed as an *in vitro* metabolic model [23] because of their unique advantages such as its richness in metabolizing enzymes, mainly CYP450 ones as well as its convenient use and the relatively low cost [24]. Indeed, pooled liver microsomes from animals or humans are mainly employed for metabolite profiling purposes as an attempt to identify any metabolic liabilities [25].

In the present study, the *in vitro* metabolism of govaniadine by CYP450 enzymes using pooled human and rat liver microsomes (HLM and RLM, respectively) was investigated. The screening of the metabolites was performed by LC–MS. The previous mentioned incubations (Sections 2.3.1 and 2.3.2) resulted in three new peaks that eluted at 3.40 (metabolite 1, M1), 4.50 (metabolite 2, M2) and 4.90 min (metabolite 3, M3), Fig. 2. They were considered to be GOV metabolites based on comparison of the control samples which were incubated in the absence of either NADPH or microsomes where no compounds were produced. The related structures were characterized on the basis of spectrometric patterns of the product ions. The mass deviation between the experimental and theoretical

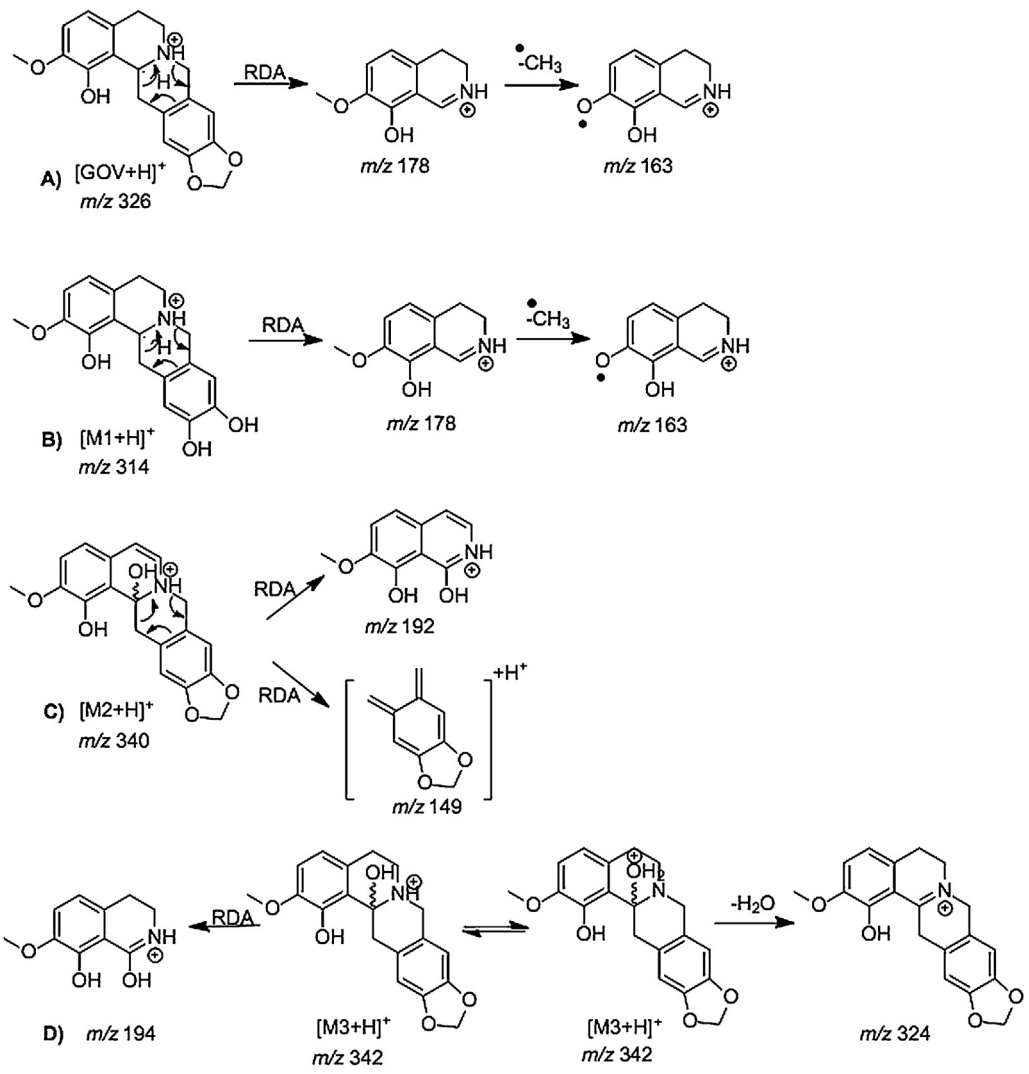

Fig. 4. Proposed fragmentation pathways of the product mass spectra of $[M+H]^+$ ions of (A) GOV, (B) M1, (C) M2 and (D) M3.

m/*z* ratio for each compound was less than 5 ppm, indicating a good correlation and providing support for the proposed elemental compositions. The characteristic MS/MS spectra of GOV metabolites are shown in Fig. 3.

Metabolite 1 (M1): It eluted with a retention time of 3.40 min (Fig. 2). It gave rise to a $[M+H]^+$ with *m*/*z* value of 314.1371 ($[C_{18}H_{20}NO_4]^+$, 4.8 ppm) (Fig. 3). The main fragment ion with *m*/*z* value of 178 was similar to those of the parent compound, corresponding to the characteristic RDA fragmentation reaction, indicating that there had been no changes to the core isoquinoline ring of govaniadine (Fig. 4B). M1 was identified as a GOV catechol-derivative, formed trough O-demethylenation. In agreement, Fraga et al. [26] demonstrated that the metabolism of a bioactive substance containing a bis-oxygenated heterocyclic ring involves the ring-cleavage and O-demethylenation to produce the respective 3,4-dihydroxyphenyl metabolite.

Metabolite 2 (M2): The mass spectra of metabolite 2 (M2), which was detected at a retention time of 4.50 min (Fig. 2), gave rise to a $[M+H]^+$ with an *m*/*z* value of 340.1171 ($[C_{19}H_{18}NO_5]^+$, 2.5 ppm). The MS/MS spectrum gave product ions with *m*/*z* value of 192 and 149 through a characteristic RDA fragmentation reaction (Figs. 3 and 4 C). The *m*/*z* 149 indicated that there had been no changes in the core of GOV tetrahydronaphthodioxole ring. M2 was tentatively proposed to be a di-hydroxylated metabolite (*m*/*z* 358). Due to an in-source dehydration, only the *m*/*z* 340 is possible to notice.

Metabolite 3 (*M3*): The mass spectra gave a protonated molecule $[M+H]^+$ with a *m*/*z* value of 342.1319 ($[C_{19}H_{20}NO_5]^+$, 4.9 ppm), which was 16 Da greater in weight than that of GOV, and it was related to a hydroxylation reaction. M3 gave product ions with *m*/*z* values of 324 and 194 (Fig. 3). The base peak at *m*/*z* 324 indicates the loss of H_2O from the $[M+H]^+$ ion and the *m*/*z* 194 was formed through a RDA reaction from the $[M+H]^+$. It is suggested that the GOV hydroxylation takes place at C(14), which tends to favor the formation of the *m*/*z* 324 by H_2O loss with only a relatively small amount of *m*/*z* 194 by a RDA reaction. Considering the hydroxylation in different positions, like C(5) or C(6), both reactions (H_2O loss and RDA) will not affect the occurrence of each one, or if it were in the positions C(8) or C(13), just one of the two reactions would be possible. Based on these data, M3 was tentatively proposed to be a mono-hydroxylated metabolite (Fig. 4D). However, the exact position of the hydroxylation could not be determined. These results show that these systems could be used to predict GOV *in vivo* metabolism.

3.3. Method development for pharmacokinetic study

In order to optimize the mass spectrometric conditions, the GOV and IS standard solutions were respectively injected into the Acquity UPLC™. MS parameters including capillary and cone voltage and collision energy were optimized to obtain the highest

Table 2
Accuracy and precision (n = 5).

Within-run				Between-run		
[Spiked](ng mL^{-1})	[Measured][a](ng mL^{-1})	RER[b],(%)	CV[c], (%)	[Measured] (ng mL^{-1})	RER,(%)	CV, (%)
2.5 (LLOQ)	2.6 ± 0.2	6	6	2.6 ± 0.2	3	9
5.0 (LQC)	4.8 ± 0.3	−3	7	5.0 ± 0.5	0	10
40.0 (MQC-1)	40.3 ± 5.8	1	14	40.1 ± 4.5	0	11
1050.0 (MQC-2)	1021.8 ± 74.1	−3	7	1051.0 ± 108.1	0	10
2630.0 (HQC)	2909.0 ± 47.9	11	2	2837.4 ± 145.6	8	5
3150.0 (ULOQ)	3446.5 ± 439.8	9	13	3214.8 ± 361.5	2	11

Legend: LQC- lower QC; MQC-1 and 2- medium QC-1 and 2; HQC- high QC; ULOQ- upper limit of quantification.
[a] Mean ± SD.
[b] Relative error, [c]coefficient of variation.

intensity for the analytes. The other parameters were adopted for the recommended value of the instrument [Fig. S2–S7 and Table S1 in (SI)]. The obtained MRM (multiple reaction monitoring) parameters are listed in Table 1.

In order to achieve the best resolution and the appropriate ionization, the chromatographic conditions including the composition of mobile phase were optimized [18]. Acetonitrile in a gradient elution was chosen and to the mobile phase was added 0.1% formic acid, to improve sensitivity and peak symmetry.

3.3.1. Sample preparation optimization

In our study, a liquid–liquid extraction (LLE) procedure was adapted from a previous work [16]. The results showed that the recovery of govaniadine was higher when ethyl acetate was employed, Fig. 5.

3.3.2. Method validation optimization

Representative MRM chromatograms of the analytes in rat plasma are shown [Fig. S8–S9 in (SI)]. As can be observed, there were no interference of endogenous compounds at the retention time of either GOV or the IS. The results indicated that when blank plasma is injected right after the calibration standard of the highest concentration (2630.0 ng mL^{-1}), there was no residue peak detected at the retention time of each analyte, which demonstrating that the carry-over effect of this method was negligible. The calibration curve was linear over the concentration range of 2.50–3150.0 ng mL^{-1} in rat plasma. The regression equation for calibration curve was y = 0.0067824x + 0.0032189 (r^2 > 0.99). The LLOQ was 2.50 ng mL^{-1} with a RER within 6.0% and a CV lower than 9.0%.

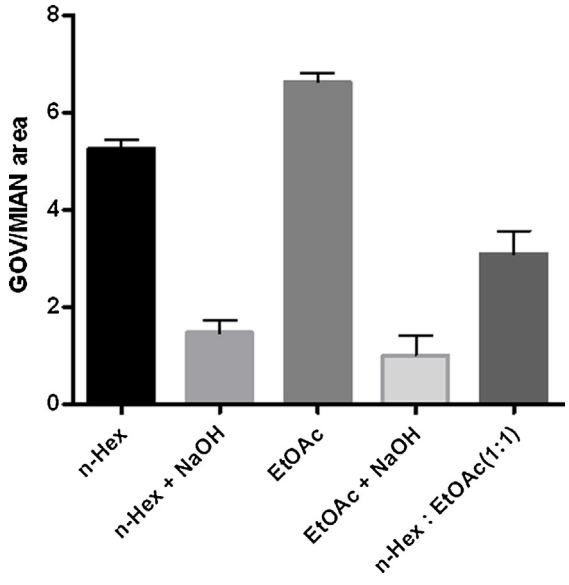

Fig. 5. Solvent evaluation for GOV extraction from plasma sample (n = 5).

Table 3
IS-normalized matrix factors at different govaniadine concentrations.

Plasma	[Spiked] (ng mL^{-1})	IS-normalized matrix factors	matrix factor (CV,%)
Normal	5	4.2 ± 0.4	8
(n = 6)	2630	1.2 ± 0.1	4
Haemolysed	5	2.5 ± 0.2	6
(n = 3)	2630	1.7 ± 0.1	6
Hyperlipidaemic	5	2.1 ± 0.0	0
(n = 3)	2630	1.6 ± 0.1	8

Regarding the precision and accuracy (within and between-run) the results are shown in Table 2. The obtained values were all within the acceptable variability limits [14], demonstrating feasibility of the method.

The GOV extraction recoveries in rat plasma ranged from 73.2 ± 3.1% to 98.1 ± 3.9% [Table S2 in (SI)] with the CV less than 4%, and the extraction efficiency of IS was 79.2 ± 8.8%. The matrix effect was evaluated by IS-normalized matrix factors (MF) using two concentration levels (5.0 and 2630.0 ng mL^{-1}). The CVs of the IS-normalized MF were less than 15%, this results indicating that matrix effects for the analytes under current method validation conditions were negligible (Table 3). The results for stability experiments are summarized in Table 4, and they showed that govaniadine was stable in rat plasma and in processed samples under all tested conditions.

3.3.3. Pharmacokinetic study

The validated LC–MS/MS method was successfully applied to a pharmacokinetic study to determine the GOV concentration in rat plasma after intravenous administration (dose = 1 mg kg^{-1}). The mean plasma concentration versus time profile is shown in Fig. 6 [Fig. S10 in (SI)]. In addition, the corresponding pharmacokinetic parameters are presented in Table 5. As can be seen the relationship between areas (r areas) was higher than 96%, demonstrating that the collection time was enough to contemplate a minimum of 80% animal exposure to GOV dose [27] and thus the experimental design was suitable for the reliable calculation of pharmacokinetic parameters. The profile was best fitted to a two-compartment model with two distinct phases. The first one (distribution) is related to a rapid decline in the GOV plasma concentration from the central compartment, with a high distribution rate constant (α) 0.139 ± 0.086 min^{-1}, which is reflected by the short distribution half-life ($t_{1/2}\alpha$) 9.2 ± 8.9 min. After reaching the Tmax = 27.7 ± 23.9 min (time to reach maximum plasma concentration), this initial phase comes to an end and the GOV concentration declines. This gradual decline appears as the later phase (disposition), with an elimination half-life ($t_{1/2}\beta$) 55.1 ± 37.9 min.

Taking into consideration the value of the cardiac output (CO) to Wistar rat as 234 mL min^{-1}/kg (CO = 180 × weight$^{-0.19}$) and 50% of this value (117 mL min $^{-1}$kg $^{-1}$) is going to be received by the liver and by the kidneys and therefore, it can not be obtained a clearance

Table 4
Stabilities of govaniadine (n = 5).

Conditions	[Spiked] (ng mL^{-1})	[Measured][a] (ng mL^{-1})	RER[b], (%)	CV[c], (%)
Freeze-thaw	5.0	5.1 ± 0.6	3	11
(3 cycles)	2630.0	2632.9 ± 218.4	0	8
Long-term stability	5.0	5.7 ± 0.3	13	4
(−60 °C, 10 days)	2630.0	2873.7 ± 242.9	9	8
Short-term stability	5.0	4.4 ± 0.5	−12	12
(25 °C, 6 h)	2630.0	2717.9 ± 395.8	3	15
Short-term stability	5.0	5.7 ± 0.6	14	11
(25 °C, 12 h)	2630.0	2972.3 ± 85.4	13	3
autosampler	5.0	5.8 ± 0.3	15	4
	2630.0	2855.6 ± 166.9	9	6

[a] Mean ± SD.
[b] Relative error, [c]coefficient of variation.

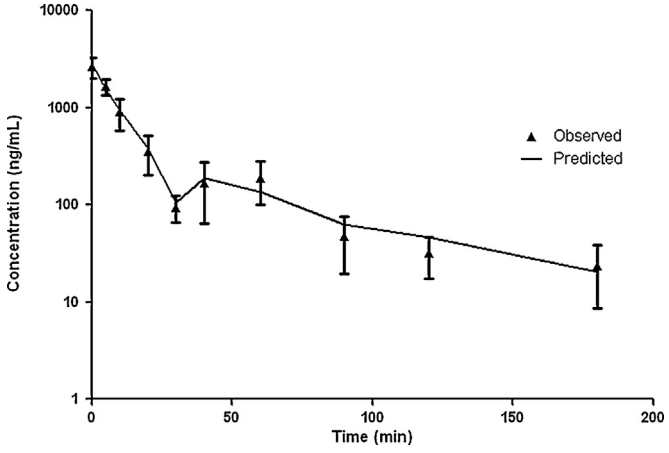

Fig. 6. Mean plasma concentration–time profiles of govaniadine in rat plasma after intravenous administration (dose = 1 mg kg^{-1}). Data are presented as observed (▲) and model predicted values (−), n = 8.

Table 5
Pharmacokinetic parameters of govaniadine in rat plasma (n = 8) after intravenous administrations (i.v.) (dose = 1 mg kg^{-1}).

Pharmacokinetic parameters	unit	i.v. (mean ± SD)
AUC_{0-t}	(min*ng mL^{-1})	42592.1 ± 37684.3
$AUC_{t-\infty}$	(min*ng mL^{-1})	44981.4 ± 41450.2
R areas	(%)	96.7 ± 2.9
β	(min^{-1})	0.017 ± 0.008
α	(min^{-1})	0.139 ± 0.086
$t_{1/2}\alpha$	(min)	9.2 ± 8.9
$t_{1/2}\beta$	(min)	55.1 ± 37.9
MRT	(min)	27.4 ± 16.4
V_d	(mL kg^{-1})	2724.3 ± 1811.4
Cl	(mL min^{-1} kg $^{-1}$)	41.7 ± 30.4
T_{max}	(min)	27.7 ± 23.9
Cp_{max}	(ng mL^{-1})	271.9 ± 216.5

greater than this, the obtained value 41.7 ± 30.4 mL min^{-1} kg $^{-1}$ is considered medium [28] which means that 17.8% of the total blood volume of the animal body that is free of the drug per minute. To the best of our knowledge, this is the first fully developed and validated LC–MS/MS method for GOV analysis in rat plasma.

3.3.4. *Protein binding ability (PPB)*

PPB is the distribution indicative of unbound drug which reflects the pharmacodynamically active drug with consequences in overall pharmacological action. The knowledge of plasma protein binding remains important throughout a drug discovery and development project, but should be integrated to pharmacokinetic data [9,18,29]. There are several *in vitro* methods for measuring the unbound fraction in plasma and, ultrafiltration is one of the most commonly used [27]. The influence of temperature in this procedure is a well-known effect for many drugs [30]. Hence, ultrafiltration at 37 °C was employed. The PPB, with NSB correction, was 92.9 ± 1.3 and 99.38 ± 0.09% for the spiked rat plasma GOV concentrations at low and high concentrations, respectively. As it was stated by Chandasana et al. [9] and Lambrinidis et al. [29] PPB can influence the clearance of drug in the body, thereby those extended PPB are probably been responsible for the medium clearance previously described. In addition, such high PPB could enable slow distribution into the intra- and extracellular space [18].

4. Conclusion

To sum up, we have demonstrated that govaniadine is metabolised by rat and human liver microsomes with the formation of three metabolites: O-demethylated, di-hydroxylated and mono-hydroxylated. The related structures were characterized on the basis of spectrometric patterns of the product ions. A sensitive, rapid and specified LC–MS/MS method was developed and successfully applied to a pharmacokinetic study of govaniadine in rats after intravenous administration. The profile was best fitted to a two-compartment model with two distinct phases. This is a first report in this field and it will be useful for further development of govaniadine as a drug candidate.

Acknowledgments

This study was supported by the Sao Paulo Research Foundation (Grants # 2013/16496-5; 2013/17658-9;2014/13192-8; 2014/23604-1) and by the National Council for Scientific and Technological Development (Grant # 442384/2014). The authors would like to express their gratitude to Prof. Dr. Cristiane Masetto Gaitani and Dr. Rodrigo Moreira da Silva (Faculdade de Ciências Farmacêuticas de Ribeirão Preto, Universidade de São Paulo) for the technical support with the protein binding assay.

Appendix A. Supplementary data

Supplementary data associated with this article can be found, in the online version, at http://dx.doi.org/10.1016/j.jpba.2016.09.003.

References

[1] J. Chen, W. Li, H. Yao, J. Xu, Insights into drug discovery from natural products through structural modification, Fitoterapia 103 (2015) 231–241.
[2] D.G.I. Kingston, Modern natural products drug discovery and its relevance to biodiversity conservation, J. Nat. Prod. 74 (2011) 496–511.
[3] J.L. Wolfender, G. Marti, A. Thomas, S. Bertrand, Current approaches and challenges for the metabolite profiling of complex natural extracts, J. Chromatogr. A 1382 (2015) 136–164.
[4] N. Muhammad, R.L. Shrestha, A. Adhikari, A. Wadood, H. Khan, A.Z. Khan, F. Maione, N. Mascolo, V. Feo, First evidence of the analgesic activity of

govaniadine, an alkaloid isolated from *Corydalis govaniana* Wall, Nat. Prod. Res. 29 (2015) 430–437.
[5] K.H. Kim, S.U. Choi, K.R. Lee, Turtschamide, a cytotoxic putrescine bisamide from *Corydalis turtschaninovii*, Tetrahedron Lett. 53 (2012) 1490–1492.
[6] Z.Y. Yang, B.H. Jiang, F.K. Teng, N. Han, Z.H. Liu, J.J. Zhou, Y. Wang, D.A. Guo, J. Yin, Ambiguanine A-G, hexahydrobenzophenanthridine alkaloids from Corydalis ambigua var. amurensis, Phytochemistry 105 (2014) 158–163.
[7] R.L.S. Shrestha, A. Adhikari, B.P. Marasini, R.N. Jha, M. Choudhary, Novel inhibitors of urease from *Corydalis govaniana* Wall, Phytochem. Lett. 6 (2013) 228–231.
[8] D.R. Callejon, T.B. Riul, L.G.P. Feitosa, T. Guaratini, D.B. Silva, A. Adhikari, R.L.S. Shrestha, L.M.M. Marques, M.D. Baruffi, J.L.C. Lopes, N.P. Lopes, Leishmanicidal evaluation of tetrahydroprotoberberine and spirocyclic erythrina-alkaloids, Molecules 19 (2014) 5692–5703.
[9] H. Chandasana, Y.S. Chhonker, V. Bala, Y.D. Prasad, T.K. Chaitanya, V.L. Sharma, R. Bhatta, Pharmacokinetic bioavailability, metabolism and plasma protein binding evaluation of NADPH-oxidase inhibitor apocynin using LC–MS/MS, J. Chromatogr. B 985 (2015) 180–188.
[10] K. He, M. Qian, H. Wong, S.A. Bai, B. He, B. Brogdon, J.E. Grace, B. Xin, J. Wu, S.X. Ren, H. Zeng, Y. Deng, D.M. Graden, T.V. Olah, E.U. Steve, J.M. Luettgen, R.M. Knabb, D.J. Pinto, P.Y.S. Lam, J. Duan, R.R. Wexler, C.P. Decicco, D.D. Christ, S.J. Grossman, N-in-1 dosing pharmacokinetics in drug discovery: experience, theoretical and practical considerations, J. Pharm. Sci. 97 (2008) 2568–2580.
[11] W. Chen, S.C.M. Yeo, X.F. Chuang, H.S. Lin, Determination of pinostilbene in rat plasma by LC–MS/MS: application to a pharmacokinetic study, J. Pharm. Biomed. Anal. 120 (2016) 316–321.
[12] N.M. Njuguna, C. Masimirembwa, K. Chibale, Identification and characterization of reactive metabolites in natural products-driven drug discovery, J. Nat. Prod. 75 (2012) 507–513.
[13] L.M.M. Marques, E.A. Silva-Junior, D.R. Gouvea, R. Vessecchi, M.T. Pupo, N.P. Lopes, M.J. Kato, A.R.M. de Oliveira, *In vitro* metabolism of the alkaloid piplartine by rat liver microsomes, J. Pharm. Biomed. Anal. 95 (2014) 113–120.
[14] European Medicines Agency (EMEA), Guideline on Bioanalytical Method Validation, 2011, http://www.ema.europa.eu/docs/en_GB/document_library/Scientific_guideline/2011/08/WC500109686. pdf (accessed 06.04.16).
[15] S. Neervannan, Preclinical formulations for discovery and toxicology: physicochemical challenges, Expert Opin. Drug Metab. Toxicol. 2 (5) (2006) 715–731.
[16] Y. Gao, S. Hu, M. Zhang, L. Li, Y. Lin, Simultaneous determination of four alkaloids in mice plasma and brain by LC–MS/MS for pharmacokinetic studies after administration of Corydalis Rhizoma and Yuanhu Zhitong extracts, J. Pharm. Biomed. Anal. 92 (2014) 6–12.
[17] R. Mukkavilli, J. Pinjari, B. Patel, S. Sengottuvelan, S. Mondal, A. Gadekar, M. Verma, J. Patel, L. Pothuri, G. Chandrashekar, P. Koiram, T. Harisudhan, A. Moinuddin, D. Launay, N. Vachharajani, V. Ramanathan, D. Martin, *In vitro* metabolism disposition, preclinical pharmacokinetics and prediction of human pharmacokinetics of DNDI-VL-2098, a potential oral treatment for visceral Lleishmaniasis, Eur. J. Pharm. Sci. 65 (2014) 147–155.
[18] J. Chen, H. Wu, G.B. Xu, M.M. Dai, S.L. Hu, L.L. Sun, W. Wang, R. Wang, S.P. Li, G.Q. Li, Determination of geniposide in adjuvant arthritis rat plasma by ultra-high performance liquid chromatography tandem mass spectrometry and its application to oral bioavailability and plasma protein binding, J. Pharm. Biomed. Anal. 108 (2015) 122–128.
[19] K.J. Lee, R. Mower, T. Hollenbeck, J. Castelo, N. Johnson, P. Gordon, P.J. Sinko, K. Holme, Y.H. Lee, Modulation of nonspecific binding in ultrafiltration protein binding studies, Pharm. Res. 20 (2003) 1015–1021.
[20] C. Lee, W. Yang, R.G. Parr, Development of the Colle-Salvetti correlation-energy formula into a functional of the electron density, Phys. Rev. B 37 (1988) 785–789.
[21] K. Cardozo, R. Vessecchi, V.M. Carvalho, E. Pinto, P.J. Gates, P. Colepicolo, S.E. Galembeck, N.P. Lopes, A theoretical and mass spectrometry study of the fragmentation of mycosporine-like amino acids, Int. J. Mass Spectrom. 273 (2008) 11–19.
[22] K. Resham, P.N. Patel, D. Thummuri, L. Guntuku, V. Shah, R.B. Bambal, V.G.M. Naidu, Preclinical drug metabolism and pharmacokinetics of salinomycin, a potential candidate for targeting human cancer stem cells, Chem. Biol. Interact. 240 (2015) 146–152.
[23] L. Yuan, P. Jia, Y. Sun, C. Zhao, X. Zhi, N. Sheng, L. Zhang, Study of in vitro metabolism of m-nisoldipine in human liver microsomes and recombinant cytochrome P450 enzymes by liquid chromatography–mass spectrometry, J. Pharm. Biomed. Anal. 97 (2014) 65–71.
[24] L. Di, C. Keefer, D.O. Scott, T.J. Strelevitz, G. Chang, Y.A. Bi, Y. Lai, J. Duckworth, K. Fenner, M.D. Troutman, R.S. Obach, Mechanistic insights from comparing intrinsic clearance values between human liver microsomes and hepatocytes to guide drug design, Eur. J. Med. Chem. 57 (2012) 441–448.
[25] J.S. Jeon, S.J. Oh, J.Y. Lee, C.S. Ryu, Y.M. Kim, B.H. Lee, S.K. Kim, Metabolic characterization of *meso*-dihydroguaiaretic acid in liver microsomes and in mice, Food Chem. Toxicol. 76 (2015) 94–102.
[26] A.G.M. Fraga, L.L. Silva, C.A.M. Fraga, E.J. Barreiro, CYP1A2-mediated biotransformation of cardioactive 2-thienylidene-3,4-methylenedioxybenzoylhydrazine (LASSBio-294) by rat liver microsomes and human recombinant CYP enzymes, Eur. J. Med. Chem. 46 (2011) 349–355.
[27] J. Fan, I.A.M. de Lannoy, Pharmacokinet. Biochem. Pharmacol. 87 (2014) 93–120.
[28] P.L. Toutain, A. Bousquet-Melou, Plasma clearance, J. Vet. Pharmacol. Ther. 27 (2004) 415–425.
[29] G. Lambrinidis, T. Vallianatou, A.T. Kakoulidou, In vitro in silico and integrated strategies for the estimation of plasma protein binding. A review, Adv. Drug Delivery Rev. 86 (2015) 27–45.
[30] V. Stove, L. Coene, M. Carlier, J.J. De Waele, T. Fiers, A.G. Verstraete, Measuring unbound versus total vancomycin concentrations in serum and plasma: methodological issues and relevance, Ther. Drug Monit. 37 (2015) 180–187.